Development 136, 2363-2373 (2009) doi:10.1242/dev.037556

Identification of *Dlk1*, *Ptpru* and *Klhl1* as novel Nurr1 target genes in meso-diencephalic dopamine neurons

Frank M. J. Jacobs[1], Annemarie J. A. van der Linden[1], Yuhui Wang[2], Lars von Oerthel[1], Hei Sook Sul[2], J. Peter H. Burbach[1] and Marten P. Smidt[1,*]

The orphan nuclear receptor Nurr1 is essential for the development of meso-diencephalic dopamine (mdDA) neurons and is required, together with the homeobox transcription factor Pitx3, for the expression of genes involved in dopamine metabolism. In order to elucidate the molecular mechanisms that underlie the neuronal deficits in *Nurr1*$^{-/-}$ mice, we performed combined gene expression microarrays and ChIP-on-chip analysis and thereby identified *Dlk1*, *Ptpru* and *Klhl1* as novel Nurr1 target genes in vivo. In line with the previously described cooperativity between Nurr1 and Pitx3, we show that the expression of *Ptpru* and *Klhl1* in mdDA neurons is also dependent on Pitx3. Furthermore, we demonstrate that Nurr1 interacts with the *Ptpru* promoter directly and requires Pitx3 for full expression of *Ptpru* in mdDA neurons. By contrast, the expression of *Dlk1* is maintained in *Pitx3*$^{-/-}$ embryos and is even expanded into the rostral part of the mdDA area, suggesting a unique position of *Dlk1* in the Nurr1 and Pitx3 transcriptional cascades. Expression analysis in *Dlk1*$^{-/-}$ embryos reveals that *Dlk1* is required to prevent premature expression of *Dat* in mdDA neuronal precursors as part of the multifaceted process of mdDA neuronal differentiation driven by Nurr1 and Pitx3. Taken together, the involvement of Nurr1 and Pitx3 in the expression of novel target genes involved in important neuronal processes such as neuronal patterning, axon outgrowth and terminal differentiation, opens up new avenues to study the properties of mdDA neurons during development and in neuronal pathology as observed in Parkinson's disease.

KEY WORDS: Developmental pathways, Dopamine, mdDA, Midbrain, Terminal differentiation, Mouse

INTRODUCTION

The orphan nuclear receptor Nurr1 (Nr4a2) was first discovered by Law et al. (Law et al., 1992) and was found to be expressed in the meso-diencephalic dopaminergic (mdDA) neurons of the substantia nigra (SNc) and ventral tegmental area (VTA) during developmental and adult stages (Zetterström et al., 1996). The first proof of a critical role for Nurr1 in the development of mdDA neurons was provided through analysis of *Nurr1*-null mouse embryos, which completely lack expression of tyrosine hydroxylase (*Th*) during development (Zetterström et al., 1997; Saucedo-Cardenas et al., 1998). Subsequent studies in *Nurr1*-null embryos added *Dat* (*Slc6a3*), *Vmat2* (*Slc18a2*), *Aadc* (*Ddc*) and *Ahd2* (*Aldh1a1*) to the list of genes that are dependent on Nurr1 for developmental expression in mdDA neurons (Wallen et al., 1999; Smits et al., 2003; Jacobs et al., 2009). Interestingly, other important developmental regulators in mdDA neurons, such as the engrailed genes *En1*/*2*, *FoxA2* (*Hnf3b*), *Lmx1b* and *Pitx3*, were still expressed in *Nurr1*-null embryos, pointing to the existence of multiple parallel pathways that act together to build a healthy mdDA population (Saucedo-Cardenas et al., 1998; Smidt et al., 2000; Wallen et al., 1999; Smits et al., 2003).

Despite the observed gene expression deficits, the generation and distribution of mdDA neuronal progenitors to their ventral positions within the mdDA area are largely unaffected in *Nurr1*$^{-/-}$ embryos (Castillo et al., 1998; Witta et al., 2000; Simon et al., 2003; Smits et al., 2003). However, defects in neuronal migration, patterning and axonal outgrowth of mdDA neurons in *Nurr1*$^{-/-}$ embryos have been reported (Wallen et al., 1999; Tornqvist et al., 2002). The most dramatic aspect of the Nurr1 phenotype is the progressive loss of mdDA neurons during late developmental stages of *Nurr1*$^{-/-}$ embryos. Apart from a small, scattered population in the medial part of the midbrain, the vast majority of mdDA neurons are lost in newborn mice (Saucedo-Cardenas et al., 1998; Castillo et al., 1998; Wallen et al., 1999). The mechanistic basis for the observed cellular defects in *Nurr1*-null embryos remains largely unknown. Interestingly, mice deficient for any of the known Nurr1 targets do not exhibit developmental defects in axonal outgrowth, neuronal migration or neuronal survival during development, similar to what was observed for *Nurr1*-null mice [known Nurr1 targets: *Vmat2* (Mosslehner et al., 2001; Colebrooke et al., 2006); *Dat* (Giros et al., 1996); *D2R* (*Drd2*) (Baik et al., 1995); *Th* (Zhou and Palmiter, 1995); *c-Ret* (Jain et al., 2006; Li et al., 2006; Kramer et al., 2007)]. This suggests that Nurr1 is required for the expression of other, yet to be identified factors that could be elementary to the multifaceted role of Nurr1 in mdDA neurons. We aimed to identify novel target genes of Nurr1 during terminal differentiation of mdDA neurons. Through microarray analysis of *Nurr1*$^{-/-}$ mouse embryos combined with in vivo ChIP-on-chip analysis and gene expression microarrays on Nurr1-overexpressing MN9D cells, we identified three novel Nurr1 target genes, *Dlk1*, *Ptpru* and *Klhl1*, that fail to be expressed in the mdDA area of *Nurr1*$^{-/-}$ embryos. Our results show that in addition to Nurr1, Pitx3 also regulates their expression, underlining the extensive cooperation between Nurr1 and Pitx3 in mdDA neurons. Intriguingly, we demonstrate that embryos deficient for *Dlk1* display deficits in the expression of *Dat*, suggesting a role for Dlk1 in mdDA neuronal differentiation. Taken together, by linking the neuronal pathology in *Nurr1*- and *Pitx3*-deficient embryos to genes involved in neuronal processes such as axon formation, neuronal patterning and terminal differentiation, we have opened up new avenues to study the complex developmental mechanism that underlies the generation of a healthy mdDA neuronal population.

[1]Rudolf Magnus Institute of Neuroscience, Department of Neuroscience and Pharmacology, University Medical Center Utrecht, Universiteitsweg 100, 3584 CG, Utrecht, The Netherlands. [2]Department of Nutritional Sciences and Toxicology, University of California, Berkeley, California 94720, USA.

*Author for correspondence (e-mail: m.p.smidt-2@umcutrecht.nl)

Accepted 14 May 2009

MATERIALS AND METHODS

Cell culture

MN9D-*Nurr1*$^{\text{Tet On}}$13N (MN9D) cells were cultured as described previously (Castro et al., 2001; Jacobs et al., 2007).

Animals

E14.5 *Pitx3*$^{-/-}$, *Pitx3*$^{+/+}$, *Nurr1*$^{-/-}$ and *Nurr1*$^{+/+}$ mouse embryos were obtained as described previously (Jacobs et al., 2009). Genotypes were determined by PCR as described previously (Saucedo-Cardenas et al., 1998). Heterozygous *Pitx3*$^{gfp/+}$ and *Pitx3*-deficient *Pitx3*$^{gfp/-}$ embryos were obtained and genotyped as described previously (Jacobs et al., 2009).

Microarray analysis

RNA was isolated from dissected ventral midbrains of E14.5 *Nurr1*$^{-/-}$ and *Nurr1*$^{+/+}$ embryos or from MN9D cells using Trizol according to the supplied protocol (Invitrogen). Microarray analysis was performed in triplicate and for each experimental sample a dye swap was performed to correct for dye effects. Each experimental sample consisted of pooled RNA derived from three *Nurr1*$^{-/-}$ ventral midbrains, which was hybridized to a reference pool consisting of RNA derived from ten *Nurr1*$^{+/+}$ ventral midbrains. Microarray analysis was performed as described (Roepman et al., 2005). Custom arrays containing mouse 70-mer oligos (Operon, Mouse V2 AROS) spotted onto CodeLink Activated Slides (Surmodiscs) were used for the hybridizations (ArrayExpress, A-UMCU-7 spotted according to protocol P-UMCU-34). Hybridized slides were scanned on an Agilent scanner (G2565AA) at 100% laser power, 30% PMT. After data extraction using ImaGene 8.0 (BioDiscovery), print-tip Loess normalization was performed on mean spot intensities. Data were analyzed using ANOVA (R version 2.2.1/MAANOVA version 0.98-7; http://www.r-project.org/) (Wu et al., 2002). In a fixed effect analysis, sample, array and dye effects were modeled. *P*-values were determined by a permutation F2 test, in which residuals were shuffled 5000 times globally. Genes with $P<0.05$ after family-wise error correction (or Benjamini-Hochberg correction) were considered significantly changed. ArrayExpress accession: E-TABM-711.

Semi-quantitative RT-PCR

RNA was isolated using Trizol according to manufacturer's protocol (Invitrogen). Semi-quantitative RT-PCR was performed on equal amounts of RNA (0.1 ng) using a one-step RT-PCR Kit (Qiagen) according to the supplied protocol. The following primers were used: *Ptpru*, 5′-ACTTCTGGCGGCTGGTCTAC-3′ and 5′-GCCACGTCGTAGCAG-AAATG-3′; *Klhl1*, 5′-AGGAGGTAGTGACAGGCATG-3′ and 5′-GGGTCTATGCCTTCCATCTTG-3′; *Dlk1*, 5′-GCATCTGCAAGG-ATGGCTG-3′ and 5′-AGACACTCGAAGCTCACCTG-3′; *Grb10*, 5′-CCCTAATCAGAGACTGAAG-3′ and 5′-TCACTGCAGTTTGC-ACTATG-3′; *Cart*, 5′-TGCTGCTACTGCTACCTTTG-3′ and 5′-CAG-GCTCCAGGGATAATGG-3′; *Rbm45*, 5′-AGTACCACGAGTCAGC-AGCAG-3′ and 5′-GTCAGTCAGCTGAGGATTATGT-3′; *Rab3c*, 5′-CTTTACATCTGCATTCGTCA-3′ and 5′-ATAACCTGGGCATTAT-CCCA-3′; *Tbp*, 5′-GAGAATAAGAGAGCCACGGAC-3′ and 5′-TCACATCACAGCTCCCCAC-3′. The amount of amplified DNA was determined by densitometry on a FLA5000 multi-imaging system (Fuji). Statistical analysis was performed by two-way unpaired Student's *t*-test, comparing the relative transcript levels of sodium butyrate-treated and untreated cultures.

Western blotting

Proteins were separated on NuPAGE 4-12% gradient gels (Invitrogen), transferred to Hybond-C extra (Amersham), the membranes blocked overnight in 5% milk powder in PBS at 4°C and then incubated with Nurr1 antibody (Santa Cruz E20) in PBS-T [PBS + 0.05% (v/v) Tween 20]. Blots were incubated with SuperSignal West Dura Extended Duration Substrate (Pierce) and exposed to ECL films (Pierce).

Chip-on-chip analysis

Chromatin immunoprecipitation (ChIP) was performed as described previously (Jacobs et al., 2009) according to the protocol supplied by NimbleGen. Briefly, five ventral midbrains from C57BL6-Jico E14.5 embryos were used for each ChIP using ChIP-grade Nurr1 antibodies (Santa Cruz E20). ChIP DNA was amplified using a Whole Genome Amplification Kit according to the manufacturer's protocol (Sigma) and used for ChIP-on-chip analysis (NimbleGen), in which Cy5-labeled Pitx3 and Nurr1 ChIP samples were hybridized to Cy3-labeled input chromatin on a mouse promoter two-array set (MM8). Microarray data were analyzed using SignalMap software (version 1.9, NimbleGen).

In situ hybridization (ISH)

ISH was performed as described previously (Smits et al., 2003; Smidt et al., 2004). The following digoxigenin (DIG)-labeled probes were used: *Tcf7l2*, bp 366-716 of the mouse cDNA (NM_009333); *Th*, 1142 bp of rat cDNA; *Vmat2*, bp 290-799 of mouse coding sequence (cds) (Smits et al., 2003); *Dat*, bp 789-1153 of rat cds; *Nurr1*, 3′ region of rat *Nurr1*; *En1*, 5′ region of mouse transcript; *Ahd2*, bp 568-1392 of mouse cds. Probes for *Dlk1*, *Klhl1*, *Ptpru*, *Grb10*, *Rab3c*, *Rbm45* and *Cart* were synthesized using the primers used for the semi-quantitative RT-PCR (see above).

Tissue culture

Ventral midbrains of *Pitx3*$^{gfp/+}$ and *Pitx3*$^{gfp/-}$ E13.5 embryos were dissected in L15 medium (Gibco) and cultured in Neurobasal Medium (Gibco) supplemented with 2% (v/v) B-27 supplement (Gibco), 18 mM HEPES-KOH (pH 7.5), 0.5 mM L-glutamine, 26 μM β-mercaptoethanol and 100 units/ml penicillin/streptomycin. Tissue cultures were treated with (0.6 mM) or without sodium butyrate (Sigma) for 48 hours.

FACS sorting

Cultured ventral midbrains were dissociated using a Papain Dissociation System (Worthington) and cells were sorted on a Cytopeia Influx cell sorter. Sort gates were set on forward scatter versus side scatter (live cell gate), on forward scatter versus pulse width (elimination of clumps) and on forward scatter versus fluorescence channel 1 (528/38 filter, GFP fluorescence). Cells were sorted using a 100-μm nozzle at a pressure of 15 PSI with an average speed of 7000 cells/second.

RESULTS

Identification of Nurr1-regulated genes by Nurr1 loss-of-function analysis

In order to identify novel target genes of Nurr1 in mdDA neurons we performed in vivo expression analysis on E14.5 *Nurr1*$^{-/-}$ mouse embryos. Based on the detection of truncated *Nurr1* transcripts in *Nurr1*$^{-/-}$ embryos, mdDA progenitors adopted their ventral position in the ventral midbrain mantle layer normally, whereas minor alterations in the rostrolateral population of mdDA neurons were observed (Fig. 1A). This confirms that the vast majority of mdDA progenitors were properly generated and distributed to build the mdDA neuronal field. Microarray analysis (*Nurr1*$^{-/-}$ against *Nurr1*$^{+/+}$) revealed that a total of 116 genes were significantly downregulated in *Nurr1*$^{-/-}$ embryonic midbrains (see Table S1 in the supplementary material). Several known Nurr1 target genes involved in dopamine (DA) metabolism, including *Dat*, *Ahd2*, *Th*, *Vmat2* and *Aadc*, were found amongst the 15 most-downregulated genes (Table 1 and Fig. 1B). As expected, the transcript levels of *En1*/2 and *FoxA2* were unchanged (Fig. 1C). In *Nurr1*$^{-/-}$ embryos there was an at least 25% reduction in the transcript levels of *Lhx2*, *Ptpru*, *Tcf7l2*, *Kitl*, *Ptprd*, *Klhl1*, *Tmed8* and *Dlk1* (Fig. 1C). Furthermore, the microarray analysis revealed a total of 139 upregulated genes in *Nurr1*$^{-/-}$ embryos (see Table S2 in the supplementary material). The greatest change was observed for a developmentally regulated transcript named *Rbm45*, followed by an additional 11 transcripts that were upregulated by at least 25% in *Nurr1*$^{-/-}$ embryos (Fig. 1D). Most of the differentially expressed transcripts in *Nurr1*$^{-/-}$ embryos are encoded by genes with no known association with Nurr1 or with mdDA neurons. For further analysis, additional lines of evidence would be beneficial to aid the selection of candidate genes that are likely to represent true Nurr1 target genes.

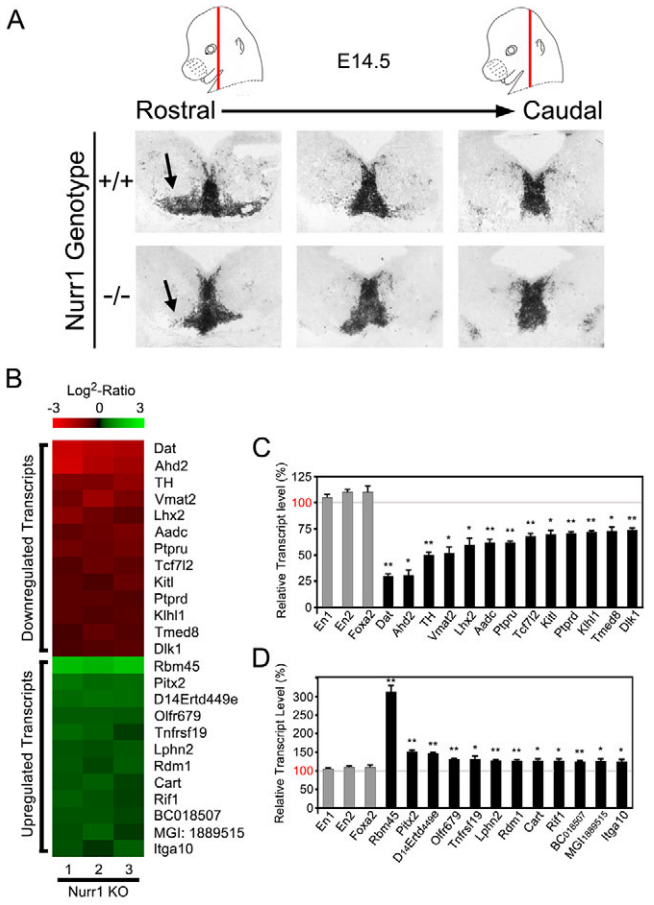

Fig. 1. Microarray analysis of *Nurr1*$^{-/-}$ mouse embryos. (**A**) Coronal sections of E14.5 *Nurr1*$^{+/+}$ (top row) and *Nurr1*$^{-/-}$ (bottom row) embryos from rostral (left) to caudal (right) positions in the midbrain. Note that *Nurr1*-truncated transcripts are still detected in *Nurr1*$^{-/-}$ embryos, showing patterning of the mdDA neuronal field except for the lateral-most population in the rostral part (arrows). (**B**) Heatmap comprising a colored representation of the $\log_2$ ratios of three individual hybridizations (*Nurr1*$^{-/-}$/*Nurr1*$^{+/+}$). Red indicates downregulation and green indicates upregulation in *Nurr1*$^{-/-}$ embryos. (**C**) The relative expression levels of transcripts showing at least 25% downregulation in *Nurr1*$^{-/-}$ embryos as compared with *Nurr1*$^{+/+}$ embryos (n=3; *, P<0.05; **, P<0.01). (**D**) Relative expression levels of transcripts showing at least 25% upregulation in *Nurr1*$^{-/-}$ embryos as compared with *Nurr1*$^{+/+}$ embryos (n=3; *, P<0.05; **, P<0.01). In C,D, gray bars indicate genes not significantly changed, black bars genes significantly changed.

In vivo ChIP-on-chip analysis reveals binding of Nurr1 to promoters of Nurr1-regulated genes

The identification of genes that are potentially under direct transcriptional control of Nurr1 is important in order to obtain a more detailed view of the hierarchical composition of the Nurr1 downstream cascade. We performed in vivo ChIP-on-chip analysis, combining chromatin immunoprecipitation (ChIP) with microarray analysis designed to identify transcription factor-bound promoters in a relatively unbiased manner (Jacobs et al., 2006). ChIP for endogenous Nurr1 protein-DNA complexes was performed on dissected tissue harboring the mdDA neurons from E14.5 C57BL6 embryos (Fig. 2A), and linearly amplified ChIP DNA fragments were hybridized to control input DNA (Fig. 2B) on an MM8 two-set promoter array. Nurr1 specifically enriched 208 promoters with a false discovery rate (FDR) of less than 0.01 (see Table S3 in the supplementary material) as described previously (Jacobs et al., 2009). Of special interest were those genes identified as Nurr1-regulated genes in *Nurr1*$^{-/-}$ mdDA neurons by the in vivo microarray analysis (Fig. 2C and Table 2). Specific enrichment by ChIP for Nurr1 was observed for the promoters of 13 genes that were significantly up- or downregulated in *Nurr1*$^{-/-}$ embryos, including the previously reported Nurr1 target gene *Vmat2* (Jacobs et al., 2009) (Fig. 2D). Of special interest was the enrichment for the promoters of *Ptpru* and *Tcf7l2* because they were in the top ten most-downregulated genes in the in vivo expression array. The ChIP-on-chip data indicate that a number of Nurr1-regulated genes are bound by Nurr1 at their promoter region in vivo, which is suggestive of direct transcriptional regulation by Nurr1.

Nurr1 gain-of-function analysis in MN9D cells

A second approach might provide additional evidence for the selection of genes that can be considered truly Nurr1 regulated in DA neurons. We analyzed the effects of *Nurr1* overexpression in DA MN9D-*Nurr1*$^{\text{Tet On}}$13N cells, which are derived from embryonic ventral midbrain tissue and modified to overexpress *Nurr1* upon treatment with doxycyclin (Fig. 3A). In agreement with previous studies (Castro et al., 2001), microarray analysis revealed that *Vmat2* was significantly upregulated in MN9D cells by *Nurr1* overexpression. Out of the set of 255 genes that showed significant changes in the in vivo expression analysis of *Nurr1*$^{-/-}$ embryos, 33 transcripts were also differentially expressed upon *Nurr1* overexpression in MN9D cells (Table 3). Interestingly, the transcript levels of *Ptpru*, *Dlk1* and *Tcf7l2*, which were all within the top 15 most-downregulated genes in vivo, were upregulated by *Nurr1* overexpression in MN9D cells (Fig. 3B). Similarly, *Grb10*, which was upregulated in *Nurr1*$^{-/-}$ embryos, was downregulated by *Nurr1* overexpression in MN9D cells. The

Table 1. The most-downregulated genes in E14.5 *Nurr1*$^{-/-}$ mouse embryos

Gene symbol	Description	$\log_2$ ratio	P-value
Dat	Dopamine transporter (*Slc6a3*)	–1.77	0.01
Ahd2	Aldehyde dehydrogenase family 1 member A1 (*Aldh1a1*)	–1.71	0.02
Th	Tyrosine hydroxylase	–1.01	0.01
Vmat2	Vesicular amine transporter 2 (*Slc18a2*)	–0.98	0.03
Lhx2	LIM homeobox protein 2	–0.76	0.04
Aadc	Aromatic-L-amino-acid decarboxylase (*Ddc*)	–0.70	0.01
Ptpru	Protein tyrosine phosphatase, receptor type, U isoform 1	–0.70	0.00
Tcf7l2	Transcription factor 7-like 2 (*Tcf4*)	–0.57	0.01
Kitl	c-Kit ligand	–0.52	0.02
Ptprd	Protein-tyrosine phosphatase delta	–0.49	0.00
Klhl1	Kelch-like protein 1	–0.47	0.00
Tmed8	Transmembrane emp24 domain containing 8	–0.47	0.02
Dlk1	Delta-like 1 protein (*Pref-1*; *FA1*)	–0.43	0.01
Avpr1a	Vasopressin V1a receptor	–0.40	0.04
Ccna2	Cyclin A2	–0.38	0.03

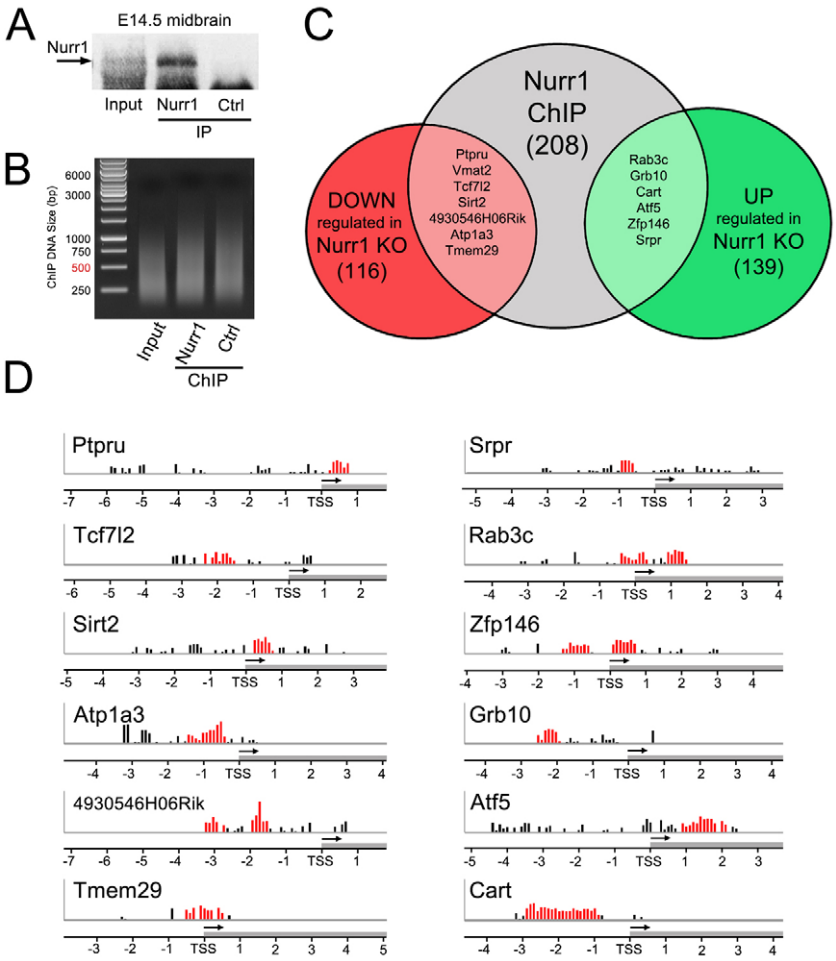

Fig. 2. ChIP-on-chip analysis identifies Nurr1 target sites in the mouse genome. (**A**) Western blot showing immunoprecipitation of endogenous Nurr1 after ChIP with Nurr1 antibodies. (**B**) DNA was sheared to an average size of 500 bp by sonication and subjected to linear amplification. (**C**) A number of genes are both differentially expressed in *Nurr1*$^{-/-}$ embryos (P<0.05) and enriched by ChIP for Nurr1 (FDR<0.01). (**D**) Nurr1 interacts with the promoters of a set of Nurr1-regulated genes. Signalmap pictures showing the relative hybridization signals of individual probes covering part of the promoter region of genes of interest as shown in C. Note that high-confidence binding sites of Nurr1 are identified by a positive signal for multiple neighboring probes (bars). The significantly Nurr1-enriched regions as identified by ChIP-on-chip are indicated as a series of red bars (a peak region). Arrows indicate gene orientation. Ctrl, control immunoprecipitation with rabbit pre-immune serum. IP, immunoprecipitation; TSS, transcription start site.

observation that these transcripts were reciprocally regulated upon *Nurr1* ablation and overexpression strongly suggests a regulatory effect of Nurr1 on these genes.

Expression of potential Nurr1-regulated genes in embryonic and adult mdDA neurons

Thus far, in vivo expression microarray analysis revealed 255 differentially expressed genes between *Nurr1*$^{+/+}$ and *Nurr1*$^{-/-}$ embryos. Thirty-three transcripts out of this set were also differentially expressed in MN9D cells upon *Nurr1* overexpression and displayed a dual dependence on Nurr1 for expression in DA neurons. Furthermore, 13 genes out of the set of deregulated transcripts in *Nurr1*$^{-/-}$ embryos were identified by ChIP-on-chip analysis as bound by endogenous Nurr1 in their promoter region. Based on these independent datasets, the following genes were selected for further analysis. *Ptpru* and *Tcf7l2* were downregulated in *Nurr1*$^{-/-}$ embryos, showed significant enrichment by ChIP for Nurr1 and were upregulated in MN9D cells by *Nurr1* overexpression. Similarly, *Grb10* and *Rab3c* were upregulated in *Nurr1*$^{-/-}$ embryos, identified by ChIP-on-chip and were differentially expressed upon *Nurr1* overexpression. *Dlk1* and *Klhl1* were amongst the 15 most-downregulated genes in *Nurr1*$^{-/-}$

Table 2. ChIP-on-chip identifies Nurr1-bound promoters of Nurr1-regulated genes in vivo

Gene symbol	Description	Peak distance to TSS	
Vmat2	Vesicular amine transporter 2 (*Slc18a2*)	–0.7	
Ptpru	Protein tyrosine phosphatase U	0.5	
Tcf7l2	Transcription factor 7-like 2 (*Tcf4*)	–1.9	
Sirt2	NAD-dependent deacetylase sirtuin 2	0.4	
Atp1a3	Na(+)/K(+) ATPase alpha-3 subunit	–0.9	
4930546H06Rik	Adult male testis cDNA	–1.7	–3.0
Tmem29	Transmembrane protein 29	0.3	
Srpr	Signal recognition particle receptor subunit alpha	–0.8	
Rab3c	Ras-related protein 3C	0.0	1.2
Zfp146	Zinc-finger protein 146	0.4	–1.0
Grb10	Growth factor receptor-bound protein 10	–2.1	
Atf5	Activating transcription factor 5	1.3	
Cart	Cocaine and amphetamine-regulated transcript	–2.4	

TSS, transcription start site.

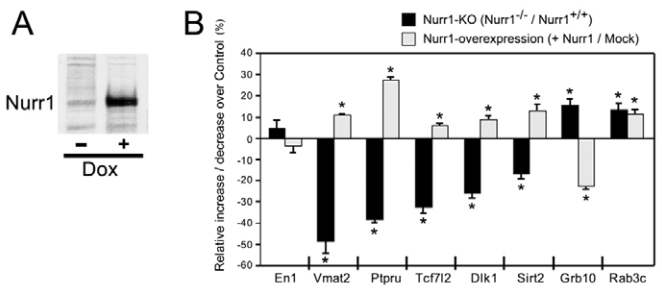

Fig. 3. Microarray analysis of Nurr1-overexpressing MN9D cells. (**A**) Western blot revealing high levels of Nurr1 protein upon treatment of MN9D-*Nurr1*$^{Tet\ On}$13N cells with doxycyclin (Dox). (**B**) The relative percentage increase or decrease of a selection of transcripts after Nurr1 overexpression (gray bars) or in *Nurr1*$^{-/-}$ embryos (black bars). *n*=3; *, *P*<0.05.

embryos, and although no evidence was found for binding of Nurr1 to their promoters, *Dlk1* was upregulated by Nurr1 in MN9D cells. *Cart* (*Cartpt*) was upregulated in *Nurr1*$^{-/-}$ embryos and was significantly enriched by ChIP for Nurr1. Finally, whereas *Rbm45* was not identified by ChIP for Nurr1, nor was it differentially expressed upon *Nurr1* overexpression in MN9D cells, *Rbm45* was selected for its high level of upregulation in *Nurr1*$^{-/-}$ embryos.

To determine whether the selected genes were expressed in the embryonic mdDA area, we performed ISH analysis on sagittal sections of wild-type (WT) E14.5 embryos (Fig. 4A-I). As discussed above, *Nurr1* was detected in the mdDA area and also in the hypothalamic nuclei located anterior to the mdDA neuronal field (Fig. 4A). *Dlk1* was expressed in the mdDA area but was clearly restricted to the caudal domain in these medial sections (Fig. 4B). A remarkably similar expression pattern was observed for *Ptpru*, which was also restricted to the caudal part of the mdDA area (Fig. 4C). Notably, the expression pattern of *Klhl1* closely resembled that of *Nurr1* at E14.5 (Fig. 4D), both being expressed in the mdDA area and in anterior neural structures such as the hypothalamus. *Tcf7l2* (Fig. 4E), *Grb10* (Fig. 4F) and *Rbm45* (Fig. 4I) were not detected in the mdDA area by ISH, and expression of *Cart* was only detected in a region dorsal to the mdDA area (Fig. 4H). Finally, *Rab3c* was clearly detected in the mdDA area, largely coinciding with the expression domain of *Nurr1*, and also in the region rostral to the mdDA area (Fig. 4G).

Although the observed expression in the mdDA domain for some of the selected genes is suggestive of expression in mdDA neurons, ISH by itself is no proof of this. Therefore, we analyzed the expression of the selected genes in FACS-sorted mdDA neurons derived from the ventral midbrain of E14.5 *Pitx3*$^{gfp/+}$ transgenic mice by RT-PCR (Fig. 4J). In agreement with what was suggested by ISH, a high level of *Dlk1*, *Ptpru*, *Klhl1* and *Rab3c* was detected in FACS-sorted *Pitx3*$^{gfp/+}$ mdDA neurons. Whereas no clear expression in the ventral midbrain was observed for *Tcf7l2*, *Grb10* and *Rbm45* by ISH, their transcripts were detected by RT-PCR, indicating that these genes are expressed in mdDA neurons but with transcript levels too low for detection by ISH. However, in agreement with the ISH data, *Cart* expression was not detected in *Pitx3*-positive mdDA neurons.

Next we analyzed the expression of the selected genes in coronal sections of the adult midbrain. Expression of *Nurr1* in mdDA neurons of the SNc and VTA was maintained in the adult (Fig. 5A).

Table 3. Genes affected by in vivo *Nurr1* deletion at E14.5 and Nurr1 overexpression in MN9D cells

	E14.5			MN9D		
Gene symbol	KO versus WT	Log_2 ratio	*P*-value	Nurr1 OE versus Ref	Log_2 ratio	*P*-value
Vmat2	Down	–0.98	0.03	Up	0.15	0.00
Lhx2	Down	–0.76	0.04	Down	–0.16	0.00
Aadc	Down	–0.70	0.01	Down	–0.30	0.01
Ptpru	Down	–0.70	0.00	Up	0.34	0.00
Tcf7l2	Down	–0.57	0.01	Up	0.08	0.01
Dlk1	Down	–0.43	0.01	Up	0.12	0.03
CcNA2	Down	–0.38	0.03	Down	–0.31	0.03
Sirt2	Down	–0.27	0.03	Up	0.18	0.04
Pde4d	Down	–0.22	0.03	Up	0.35	0.03
Eps8	Down	–0.20	0.01	Up	0.25	0.03
4930546H06Rik	Down	–0.17	0.04	Down	–0.18	0.01
Akr1b3	Down	–0.15	0.02	Down	–0.19	0.02
Mrpl38	Down	–0.15	0.00	Up	0.16	0.01
Ppm1a	Down	–0.15	0.05	Up	0.20	0.00
Fdps	Up	0.15	0.03	Down	–0.74	0.00
Auh	Up	0.15	0.01	Up	0.21	0.03
BC048507	Up	0.16	0.03	Down	–0.27	0.01
NAsp	Up	0.16	0.03	Down	–0.18	0.04
Hmgb2	Up	0.16	0.01	Down	–0.21	0.04
AW549877	Up	0.17	0.01	Up	0.26	0.01
5730403M16Rik	Up	0.17	0.03	Up	0.15	0.00
Rab3c	Up	0.18	0.04	Up	0.15	0.03
Grb10	Up	0.21	0.03	Down	–0.37	0.01
Thoc4	Up	0.21	0.05	Down	–0.20	0.04
Prpf40a	Up	0.21	0.00	Up	0.18	0.01
Dmrta2	Up	0.21	0.01	Down	–0.24	0.00
Smarce1	Up	0.22	0.05	Down	0.18	0.01
Rhoq	Up	0.24	0.02	Up	0.18	0.03
Ttc33	Up	0.25	0.04	Up	0.24	0.00
2310003F16Rik	Up	0.27	0.03	Down	–0.17	0.04
Rif1	Up	0.34	0.03	Down	–0.16	0.00

KO, *Nurr1* knockout; WT, wild type; OE, overexpression; Ref, uninduced.

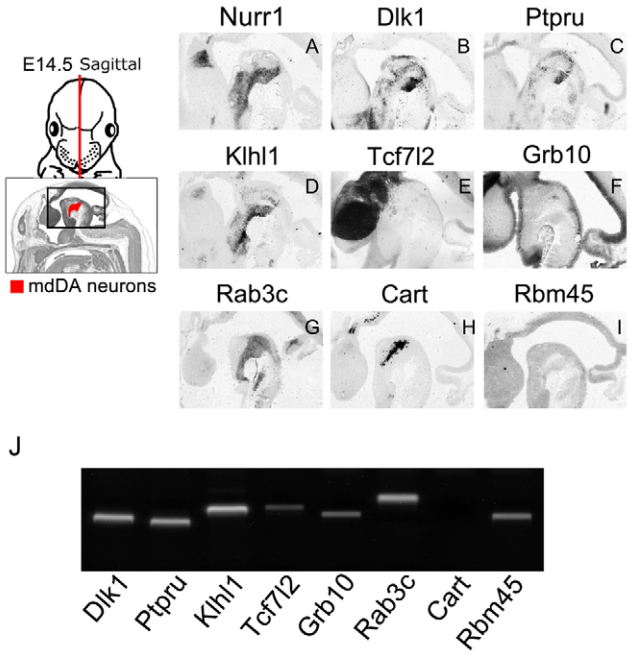

Fig. 4. Embryonic expression of potential Nurr1-regulated genes. To the left is shown a sagittal section of an E14.5 mouse embryo. The mdDA area is indicated in red and the boxed area corresponds to that shown in A-I. (**A**) Embryonic expression of *Nurr1*. (**B-I**) Embryonic expression of *Dlk1* (B), *Ptpru* (C) *Klhl1* (D) and *Rab3c* (G) was detected in the mdDA area (partly) corresponding to the *Nurr1* expression domain (A). *Tcf7l2* expression was detected outside the mdDA area (E) and *Cart* expression was detected in a region just dorsal to the mdDA area (H). No expression in the midbrain was detected for *Grb10* (F) and *Rbm45* (I). (**J**) RT-PCR on RNA derived from FACS-sorted *Pitx3*$^{gfp/+}$ mdDA neurons demonstrates relatively high transcript levels of *Dlk1*, *Ptrpu*, *Klhl1* and *Rab3c*, and low transcript levels of *Tcf7l2*, *Grb10* and *Rbm45* in mdDA neurons.

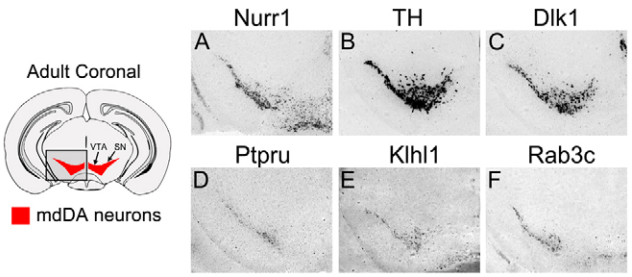

Fig. 5. Adult expression of potential Nurr1-regulated genes. To the left is shown a coronal section of the adult mouse brain. The mdDA area is indicated in red and the boxed area corresponds to that shown in A-F. (**A**,**B**) Expression of *Nurr1* (A) and *Th* (B) in the adult SNc. (**C-F**) Expression of *Dlk1* (C), *Ptpru* (D), *Klhl1* (E) and *Rab3c* (F).

Furthermore, *Dlk1* was still robustly expressed in the adult mdDA area (Fig. 5C) and its expression pattern was remarkably similar to that of *Th* (Fig. 5B). *Ptpru* was only detected in the ventral part of the SNc and its overall expression level was low (Fig. 5D). In agreement with what was observed in the embryonic midbrain, the expression pattern of *Klhl1* resembled that of *Nurr1* in both the SNc and VTA regions of the adult midbrain (Fig. 5E). A similar pattern was observed for *Rab3c* (Fig. 5F). A very low signal was detected for *Grb10* in the adult mdDA system, and no expression was observed for *Tcf7l2*, *Cart* and *Rbm45* (data not shown).

Expression of *Dlk1*, *Ptpru* and *Klhl1* is affected in *Nurr1*$^{-/-}$ embryos

Most of the selected potential Nurr1-regulated genes were expressed in the embryonic mdDA area. These observations made it most interesting to analyze the expression of this set of genes in the mdDA region of *Nurr1*$^{-/-}$ embryos. The expression of truncated *Nurr1* transcripts was used to demonstrate the presence of mdDA precursors in the *Nurr1*-deficient mdDA area (Fig. 6A,I). In agreement with the in vivo microarray analysis on *Nurr1*$^{-/-}$ embryos, the expression of *Dlk1* was substantially reduced in the mdDA area in *Nurr1*$^{-/-}$ embryos (Fig. 6B,J) and was only retained in a selective population of neurons along the midline (Fig. 6J). *Nurr1* deficiency specifically affected the mdDA neuronal population, as the expression of *Dlk1* in other structures in the brain was unaffected. Similarly, *Ptpru* expression was absent in the mdDA area of *Nurr1*$^{-/-}$ embryos, whereas *Ptpru* expression outside the mdDA area was unaffected (Fig. 6C,K). Also, the expression of *Klhl1* was clearly reduced in the *Nurr1*-null mdDA area (Fig. 6D,L). Although *Klhl1* expression was not completely absent, there was a significant decrease in expression in the area where the *Th*-positive neurons would normally reside. Importantly, *Klhl1* expression in the *Nurr1*-positive hypothalamic nuclei was unaffected by *Nurr1* deficiency. Although the microarray analysis suggested altered transcript levels in *Nurr1*$^{-/-}$ embryos, the expression of *Tcf7l2* (Fig. 6E), *Cart* (Fig. 6F), *Rab3c* (Fig. 6G) and *Grb10* (Fig. 6H) appeared to be unchanged in *Nurr1*$^{-/-}$ versus *Nurr1*$^{+/+}$ embryos. It should be noted that we cannot exclude the possibility that there are small changes in expression that are not detectable by the ISH method used. Altogether, the in vivo expression analysis revealed severe deficits in the expression of *Ptpru*, *Klhl1* and *Dlk1* in the mdDA area of *Nurr1*$^{-/-}$ embryos, indicating that they represent novel Nurr1 target genes.

Pitx3 deficiency affects expression of *Dlk1*, *Ptpru* and *Klhl1*

Previously, we have shown that Pitx3 potentiates Nurr1 in mdDA neurons, which translates to severe expression deficits of Nurr1 target genes in *Pitx3*-deficient mdDA neurons (Jacobs et al., 2009). The identification of novel Nurr1 target genes in mdDA neurons prompted us to determine whether *Pitx3* deficiency also affects the expression of these genes in the mdDA area. We analyzed the expression of *Ptpru*, *Klhl1* and *Dlk1* in *Pitx3*$^{-/-}$ embryos at E14.5. As described previously (Jacobs et al., 2009), the expression of *Nurr1* in *Pitx3*$^{-/-}$ embryos was undistinguishable from that in WT and could therefore be used to show the presence of mdDA neurons in *Pitx3*$^{-/-}$ embryos (Fig. 7A). Interestingly, the expression of *Ptpru* and *Klhl1* was dramatically reduced in *Pitx3*$^{-/-}$ embryos (Fig. 7B,C). Similar to what was previously observed for other Nurr1 target genes, *Ptpru* and *Klhl1* expression was still detected in the mdDA area of *Pitx3*$^{-/-}$ embryos, but was significantly reduced compared with WT. However, in contrast to what was observed for *Ptpru*, *Klhl1* and other Nurr1 target genes in *Pitx3*$^{-/-}$ embryos (Jacobs et al., 2009), *Dlk1* expression was still abundant in the mdDA area of *Pitx3*$^{-/-}$ embryos (Fig. 7D). Strikingly, whereas *Dlk1* expression in WT embryos was confined to the caudal part of the mdDA area, the expression domain of *Dlk1* in *Pitx3*$^{-/-}$ embryos was even expanded into anterior positions within the mdDA area (Fig. 7D, insets).

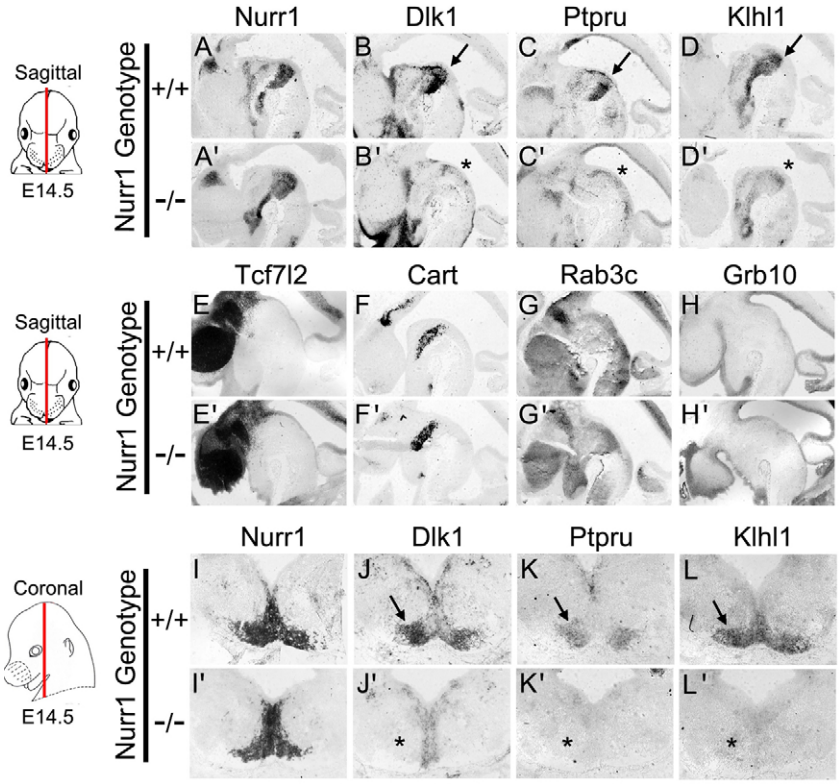

Fig. 6. Expression of potential Nurr1-regulated genes in E14.5 *Nurr1*$^{-/-}$ embryos. (**A-H'**) Sagittal sections (as illustrated to the left) of *Nurr1*$^{+/+}$ (A-H) and *Nurr1*$^{-/-}$ (A'-H') mouse embryos demonstrating expression of *Nurr1* (A), *Dlk1* (B), *Ptpru* (C), *Klhl1* (D), *Tcf7l2* (E), *Cart* (F), *Rab3c* (G) and *Grb10* (H). Note the selective deficit of expression for *Dlk1* (B'), *Ptpru* (C') and *Klhl1* (D') in the mdDA area of *Nurr1*$^{-/-}$ embryos, independent of neuronal loss at E14.5 based on the detection of truncated *Nurr1* transcripts (B'). (**I-L'**) Coronal sections of *Nurr1*$^{+/+}$ (I-L) and *Nurr1*$^{-/-}$ (I'-L') embryos demonstrating expression of *Nurr1* (I), *Dlk1* (J), *Ptpru* (K) and *Klhl1* (L). *Dlk1* expression is restricted to the midline region within the mdDA area in *Nurr1*$^{-/-}$ embryos (J'), whereas expression of *Ptpru* (K') and *Klhl1* (L') is virtually lost in the *Nurr1*-deficient mdDA area. Arrows indicate mdDA-specific endogenous gene expression that is lost (asterisks) in *Nurr1*$^{-/-}$ embryos.

We have shown previously that Pitx3 potentiates Nurr1 by inducing the release of the nuclear receptor co-repressor SMRT (Ncor2) from the Nurr1 transcriptional complex, thereby activating Nurr1 target gene expression (Jacobs et al., 2009). The requirement for Pitx3 in driving Nurr1 target gene expression could be bypassed by interfering with the SMRT/HDAC-mediated repression of Nurr1 transcriptional activity. Treatment of *Pitx3*-deficient cultured ventral midbrains with the HDAC inhibitor sodium butyrate (SB) restored the expression of Nurr1 target genes in the absence of Pitx3 (Fig. 7E). We tested whether the proposed mechanism of Pitx3/Nurr1 cooperativity is also valid for the expression of *Ptpru* and *Klhl1* in mdDA neurons. We cultured ventral midbrains of E13.5 *Pitx3*$^{gfp/-}$ and *Pitx3*$^{gfp/+}$ embryos with SB or control diluent to release the SMRT/HDAC-mediated repression of the Nurr1 transcriptional complex. Semi-quantitative RT-PCR on FACS-sorted mdDA neurons revealed that treatment with SB did not affect the expression of *Tbp* in heterozygous *Pitx3*$^{gfp/+}$ and *Pitx3*-deficient *Pitx3*$^{gfp/-}$ mdDA neurons (Fig. 7F). Furthermore, SB treatment did not affect the level of *Ptpru* transcripts in FACS-sorted *Pitx3*$^{gfp/+}$ mdDA neurons, indicating that in the presence of Pitx3, Nurr1-mediated expression of *Ptpru* is not repressed by SMRT/HDAC complexes (Fig. 7F,G; n=4). In agreement with what was observed for *Ptpru* expression by ISH, a lower level of *Ptpru* transcripts was observed in untreated *Pitx3*$^{gfp/-}$ mdDA neurons: ~48%, as compared with the level of *Ptpru* in untreated *Pitx3*$^{gfp/+}$ mdDA neurons. However, SB treatment resulted in a significant increase in *Ptpru* transcripts, restoring levels to 73% (n=4; P<0.05), indicating that in the absence of Pitx3, Nurr1-mediated expression of *Ptpru* is repressed in an HDAC-dependent manner. This further supports a direct transcriptional regulation of *Ptpru* by Nurr1, which was also suggested by our ChIP-on-chip data. Unexpectedly, SB treatment resulted in a strong decrease in *Klhl1* transcript levels in both *Pitx3*$^{gfp/+}$ and *Pitx3*$^{gfp/-}$ mdDA neurons (Fig. 7F,H; n=4). Apparently, interference with HDAC-mediated repression negatively affects *Klhl1* expression independent of the absence or presence of Pitx3. In summary, these data demonstrate that whereas *Dlk1* expression increased in the absence of Pitx3, the expression of *Ptpru* and *Klhl1* dramatically decreased in *Pitx3*$^{-/-}$ embryos. Furthermore, our data indicate that *Ptpru* is regulated by the combined action of Pitx3 and Nurr1 via the previously proposed mechanism of Pitx3-mediated potentiation of Nurr1 (Fig. 7E).

Expression of *Dat* is affected in *Dlk1*$^{-/-}$ embryos

A recent study has hinted at a role for Dlk1 in promoting the proliferation and differentiation of Th-positive neurons from in vitro cultured mdDA precursors (Bauer et al., 2008). The contrasting effects of Nurr1 and Pitx3 on the expression of *Dlk1* in mdDA neurons have evoked interest concerning the role of Dlk1 during the development of mdDA neurons in vivo. We examined the molecular and morphological consequences of *Dlk1* deficiency in *Dlk1*$^{-/-}$ embryos. All the genes tested were still expressed in the *Dlk1*-deficient mdDA area and, based on the expression pattern of *En1* at E14.5, the mdDA field was generated normally (Fig. 8A,E). Furthermore, the expression of *Th*, *Nurr1*, *Pitx3*, *Vmat2* and *Ahd2* was undistinguishable from that of WT controls (*Th*, Fig. 8B,F; *Pitx3*, Fig. 8D,H; data not shown). However, the expression pattern of *Dat* was strikingly different from that of WT. In WT embryos, *Dat* was expressed in mdDA neurons during the final stages of differentiation and was restricted to the lateral population in rostral sections (Fig. 8C). Strikingly, in rostral sections of *Dlk1*$^{-/-}$ E14.5 embryos, *Dat* was also expressed in the medial region of the mdDA area (Fig. 8C'), which is normally completely devoid of *Dat* expression. This region harbors the young mdDA precursors during their migratory phase (Shults et al., 1990; Kawano et al., 1995). This indicates that in the absence of *Dlk1*, mdDA neuronal precursors prematurely differentiate into *Dat*-positive neurons before they have reached their final positions in the mdDA area. Notably, in WT embryos, *Dat* is not expressed in all

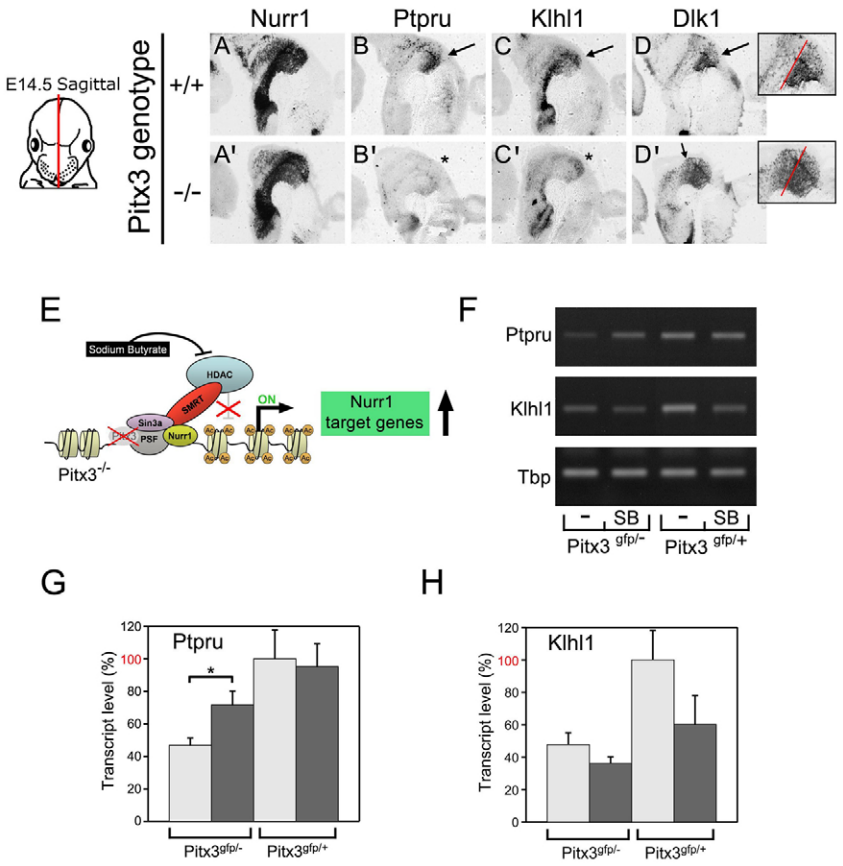

Fig. 7. Expression of *Ptpru*, *Klhl1* and *Dlk1* in E14.5 *Pitx3*$^{-/-}$ embryos. (**A-D′**) Sagittal sections of *Pitx3*$^{+/+}$ (A-D) and *Pitx3*$^{-/-}$ (A′-D′) mouse embryos demonstrating expression of *Nurr1* (A), *Ptpru* (B), *Klhl1* (C) and *Dlk1* (D). Expression of *Ptpru* (B′) and *Klhl1* (C′) was dramatically decreased whereas *Dlk1* expression was expanded in the anterior direction (D′) in the *Pitx3*$^{-/-}$ mdDA area. Arrows indicate endogenous expression and asterisks indicate deficit of expression in *Nurr1*$^{-/-}$ embryos. Insets in D,D′ are magnifications of the mdDA area; the red line represents the virtual border separating the caudal and rostral expression of Dlk1. (**E**) Previously described model of SMRT/HDAC-mediated repression of Nurr1 transcriptional activity in *Pitx3*-deficient mdDA neurons, resulting in decreased levels of expression of Nurr1 target genes in the absence of Pitx3 (Jacobs et al., 2009). (**F-H**) Semi-quantitative RT-PCR on RNA derived from FACS-sorted *Pitx3*$^{gfp/-}$ or *Pitx3*$^{gfp/+}$ mdDA neurons after treatment with either the HDAC inhibitor sodium butyrate (SB) or control diluent. (F,G) Relative transcript levels of *Ptpru* in *Pitx3*$^{gfp/-}$ and *Pitx3*$^{gfp/+}$ mdDA neurons upon treatment with SB or control diluent (–) (n=4; *, P<0.05). (F,H) Relative transcript levels of *Klhl1* in *Pitx3*$^{gfp/-}$ and *Pitx3*$^{gfp/+}$ mdDA neurons upon treatment with SB or control diluent (–) (n=4). In G,H, light-gray bars indicate untreated cells and dark-gray bars cells treated with SB.

differentiated mdDA neurons, and is predominantly expressed in DA neurons of the SNc (Hurd et al., 1994). Indeed, in E14.5 WT embryos, the caudal (VTA) part of the mdDA area was clearly devoid of *Dat* expression (Fig. 8G). However, in *Dlk1*$^{-/-}$ embryos, *Dat* was highly expressed in this part of the mdDA area (Fig. 8G′), suggesting that Dlk1 might repress *Dat* in DA neurons of the VTA.

Further analysis revealed that *Dat* was ectopically expressed in other regions of the *Dlk1*-deficient embryonic brain. Whereas *Dat* expression was highly restricted to the mdDA area in WT embryos (Fig. 8I,M), *Dlk1*$^{-/-}$ embryos showed ectopic expression of *Dat* in the thalamus (Fig. 8J) and hindbrain (Fig. 8N). Notably, these neuronal tissues were positive for both *Nurr1* (Fig. 8K,O) and *Dlk1* (Fig. 8L,P) transcripts in WT embryos. These observations indicate that Nurr1-mediated induction of *Dlk1* might be necessary to repress *Dat* expression in neuronal cell types other than DA neurons of the SNc. Although these observations suggest a role for Dlk1 in the timing and fine-tuning of *Dat* expression in the mdDA area and other neural structures at E14.5, we did not observe differences in *Dat* expression at E18.5, nor did we detect any molecular or morphological alterations of the mdDA area when compared with WT controls at this stage (data not shown). Altogether, the molecular analysis of the mdDA area in *Dlk1*$^{-/-}$ embryos suggests an inhibitory role for Dlk1 in the expression of *Dat* at E14.5, which is reflected in premature expression in precursors of SNc neurons, misexpression of *Dat* in the caudal (VTA) part of the mdDA area, and ectopic expression of *Dat* in other *Nurr1*-positive structures in the absence of *Dlk1*.

Taken together, we have established *Dlk1*, *Ptpru* and *Klhl1* as novel targets of the Nurr1 and Pitx3 downstream cascades in the mdDA neuronal population. The involvement of these genes in neuronal processes that are affected in *Nurr1*$^{-/-}$ embryos provides novel clues as to the molecular basis for some aspects of the multifaceted role of Nurr1 in mdDA neurons (Fig. 9).

DISCUSSION

Novel targets of Nurr1 and Pitx3 in mdDA neurons

Nurr1 is best known for its role in promoting the DA phenotype of mdDA neurons, leading to expression deficits of multiple DA-related genes upon genetic deletion of *Nurr1*. The involvement of Nurr1 in the DA phenotype only partially reflects the complex role of this protein in mdDA neurons, as other developmental defects in *Nurr1*$^{-/-}$ embryos have remained unexplained. These include mdDA-specific neuronal loss, defective formation of nerve fiber bundles and defects in neuronal migration and patterning. We hypothesized that Nurr1 might regulate additional target genes or molecular cascades that could further elucidate the role of Nurr1 during mdDA development. In this study, we identified *Dlk1*, *Ptpru* and *Klhl1* as novel target genes of Nurr1 in vivo. In agreement with a cooperative function of Pitx3 and Nurr1 in mdDA neurons, the expression of *Ptpru* and *Klhl1* was also severely affected in *Pitx3*$^{-/-}$ mdDA neurons. Whereas the co-regulatory effect of Nurr1 and Pitx3 is observed for most Nurr1 target genes, the regulation of *Dlk1* in mdDA neurons appears to be the exception to the rule.

The role of Klhl1 in mdDA neurons

Klhl1 is primarily expressed in the brain (Chen et al., 2008), and we showed for the first time that the expression pattern of *Klhl1* strongly resembles that of *Nurr1* in the mdDA area and other *Nurr1*-positive structures. *Klhl1* is the homolog of the actin-organizing *kelch* gene in

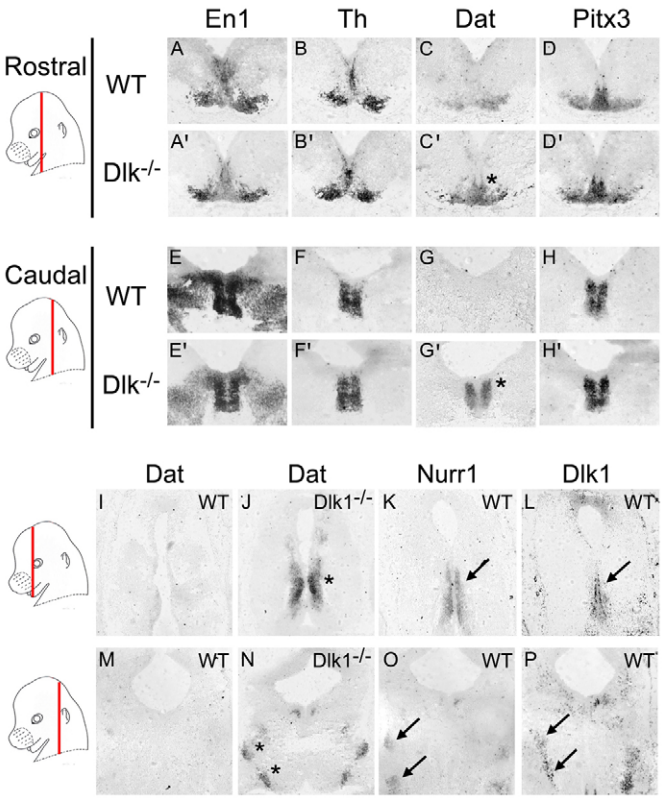

Fig. 8. The role of Dlk1 during mdDA neuronal differentiation. (**A-H′**) Coronal sections of the rostral (A-D) and caudal (E-H) mdDA area of wild-type (WT) (A-H) and *Dlk*$^{-/-}$ (A′-H′) E14.5 mouse embryos. There is normal expression of *En1* (A,E) and *Th* (B,F) but abnormal expression of *Dat* in the medial region of the rostral (C′) and caudal (G′) mdDA area of *Dlk1*$^{-/-}$ embryos, corresponding to the region where *Pitx3* is expressed (D,H). (**I-P**) Coronal sections of the thalamic (I-L) and hindbrain (M-P) area showing lack of *Dat* expression in WT embryos (I,M) and ectopic expression of *Dat* in *Dlk1*$^{-/-}$ embryos (J,N) at E14.5. *Dat* is ectopically expressed in tissues positive for *Nurr1* (K,O) and *Dlk1* (L,P) in WT embryos. Asterisks indicate abnormal *Dat* expression and arrows indicate expression of *Nurr1* and *Dlk1*.

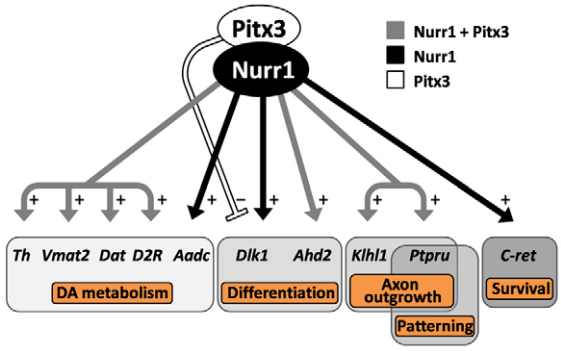

Fig. 9. Model of gene activation by Nurr1 and Pitx3 in mdDA neurons. Nurr1 and Pitx3 regulate genes involved in DA metabolism, terminal differentiation, axon outgrowth, neuronal patterning and survival. Gray arrows indicate concerted regulation by Nurr1 and Pitx3. Black arrows indicate regulation by Nurr1. The white arrow indicates regulation by Pitx3. +, positive effect on expression; –, negative effect on expression.

Drosophila (Nemes et al., 2000) and is described as playing a central role in neurite outgrowth (Seng et al., 2006). In line with this role, *Klhl1*-null mice exhibit deficits in neurite formation of Purkinje cells (He et al., 2006) and display abnormal gait and progressive loss of motor coordination. Although these Parkinson-like symptoms are most intriguing in view of the association of Klhl1 with mdDA neuronal pathology, they have been mainly attributed to *Klhl1*-related deficits in Purkinje cells of the cerebellum (He et al., 2006). However, in humans, a direct link between abnormal expansions of trinucleotide repeats within the *SCA8* locus, where *KLHL1* is located, and cases of Parkinson's disease have been reported (Worth et al., 2000; Izumi et al., 2003; Wu et al., 2004). The expression of *Klhl1* in mdDA neurons of the SNc and VTA and the notion that *Klhl1* is linked to mdDA pathology in *Nurr1*- and *Pitx3*-deficient embryos provide a new basis for studying the role of *Klhl1* in the mdDA system.

The involvement of Ptpru in Wnt signaling in mdDA neurons

Ptpru expression in mdDA neurons requires both Pitx3 and Nurr1 and we provided evidence for a direct transcriptional regulation of *Ptpru* by their combined action. Receptor-type protein tyrosine phosphatases (PTPRs), like Ptpru, dephosphorylate tyrosine residues on target proteins, thereby counteracting the activity of protein tyrosine kinases (Stoker and Dutta, 1998). Reversible protein phosphorylation is an essential mechanism to regulate intracellular signaling cascades. The central role of PTPRs in determining the intensity and duration of multiple signaling cascades implicates PTPRs in multiple cellular processes in the brain (Paul and Lombroso, 2003). Previously, PTPRs have been implicated in axonal growth and guidance (Stepanek et al., 2005) and Ptpru is directly involved in Wnt signaling through binding and sequestering β-catenin (Yan et al., 2002; Yan et al., 2006; Badde and Schulte, 2008). Intriguingly, the Ptpru ortholog in chick has been implicated in patterning of the ventral midbrain (Badde et al., 2005; Badde and Schulte, 2008). Through a series of elegant studies, the authors showed that Ptpru is intimately linked to Fgf8 and Wnt signaling in the ventral midbrain area. Ptpru exhibited a repressive effect on the expression of *Wnt1*, which is a crucial factor for proliferation and patterning of the mdDA neuronal field (Megason and McMahon, 2002). In line with this role, overexpression of Ptpru had an anti-proliferative effect on DA progenitors (Badde and Schulte, 2008). These data indicate an important role for Ptpru in patterning of the chick midbrain. Our analysis revealed that Ptpru continues to be expressed in the mdDA area during terminal differentiation and into adulthood, suggesting that this is not the only role for Ptpru.

Evidence for a role of Dlk1 in mdDA neuronal differentiation

Dlk1 was expressed in the embryonic mdDA area and its expression was maintained to a high level in the adult. We showed that *Dlk1* expression was largely abolished in the mdDA area in *Nurr1*$^{-/-}$ embryos. *Dlk1* encodes a transmembrane protein containing six EGF repeats and is mainly described for its role in the differentiation of adipocytes and osteoblasts (Moon et al., 2002; Abdallah et al., 2004). Continued expression of *Dlk1* in cultured adipocytes is inhibitory to differentiation (Enomoto et al., 2004) and differentiation of pre-adipocytes to mature adipocytes is preceded by downregulation of *Dlk1* (Hansen et al., 1998; Smas et al., 1999). Although *Dlk1* was previously shown to be expressed in Th-positive neurons of the SNc and VTA, its role in mdDA neurons is largely unknown (Jensen et al., 2001; Christopherson et al., 2007). In vitro studies on ventral midbrain-derived precursors of DA neurons revealed that treatment

with Dlk1 protein during expansion of the primary culture increased DA precursor proliferation, whereas treatment during DA neuron differentiation did not alter the number of Th-positive neurons. However, interference with *Dlk1* expression during differentiation resulted in decreased levels of a subset of mdDA markers, which suggested a permissive role for Dlk1 in the terminal differentiation of mdDA precursors in vitro (Bauer et al., 2008).

To examine the role of Dlk1 in the development of mdDA neurons in vivo, we analyzed the mdDA area in *Dlk1*$^{-/-}$ mice. Strikingly, whereas *Dat* expression is restricted to the rostrolateral population of differentiated mdDA neurons in WT embryos, *Dat* was abnormally expressed in the medial region of the rostral mdDA area of *Dlk1*$^{-/-}$ embryos. This region harbors mdDA precursors that are migrating ventrally to their final positions in the mantle layer (Shults et al., 1990; Kawano et al., 1995). The expression of *Dat* in these mdDA precursors suggests a premature differentiation into *Dat*-positive neurons in the absence of *Dlk1*. Furthermore, in *Dlk1*$^{-/-}$ embryos, *Dat* was expressed in the mdDA area harboring the DA neurons of the VTA, whereas this area is largely devoid of *Dat* expression in WT embryos. This suggests that Dlk1 is important to repress *Dat* expression in mdDA neurons of the VTA, which might be fundamental to the relatively restricted expression of *Dat* in mdDA neurons of the SNc in WT embryos. In addition to the aberrant expression of *Dat* in the mdDA area, *Dat* was ectopically expressed in Nurr1/Dlk1-positive tissues in the thalamus and hindbrain. It should be noted that in line with previous reports (Moon et al., 2002), we observed a partial penetrance of the phenotype, as not all embryos displayed the aberrant expression pattern of *Dat*. Altogether, these data indicate an inhibitory role for Dlk1 in Nurr1-mediated expression of *Dat*, an important intrinsic regulator of the timing and cell type specificity of *Dat* expression in the brain. Notably, our in vivo data did not support a permissive role for Dlk1 in the differentiation of mdDA neurons in vitro (Bauer et al., 2008). By contrast, our in vivo data point to the premature expression of *Dat* in mdDA progenitors in the absence of *Dlk1*, which is in line with the suppressive role of Dlk1 in the differentiation of many non-neuronal tissues (Enomoto et al., 2004; Abdallah et al., 2004; Hansen et al., 1998; Smas et al., 1999). Although the exact mechanism remains to be clarified, our present data provide evidence of an important role for Dlk1 in the development of mdDA neurons in vivo.

In conclusion, the identification of *Klhl1*, *Ptpru* and *Dlk1* as novel downstream targets of Nurr1 has provided further insight into its multifaceted role in the mdDA neuronal population. We have established Nurr1 as an essential regulator of genes that are involved in neuronal processes such as axonal outgrowth, neuronal patterning and terminal differentiation, processes that are also affected in *Nurr1*$^{-/-}$ embryos (Fig. 9). Therefore, our data might form the molecular basis for a subdivision of the Nurr1 downstream cascade into several distinctive pathways, each accounting for separate aspects of the complex phenotype of mdDA neurons in *Nurr1*$^{-/-}$ embryos. The connection of at least one of the newly described Nurr1 target genes with mdDA neuronal differentiation in vivo underlines the importance of identifying novel players and pathways in mdDA neurons in order to obtain a detailed view of the developmental properties of these neurons in health and disease.

Acknowledgements

We thank Marian Groot Koerkamp for the microarray analysis, Thomas Perlmann for providing MN9D cells, Orla Conneely for providing *Nurr1*-null mice, Meng Li for providing Pitx3-GFP knock-in mice, Ger Arkestein for FACS sorting and Roger Koot for assistance with data analysis. This work was supported by an HIPO grant (University of Utrecht) and by a NWO VICI grant (865.09.002) to M.P.S.

Supplementary material

Supplementary material for this article is available at http://dev.biologists.org/cgi/content/full/136/14/2363/DC1

References

Abdallah, B. M., Jensen, C. H., Gutierrez, G., Leslie, R. G., Jensen, T. G. and Kassem, M. (2004). Regulation of human skeletal stem cells differentiation by Dlk1/Pref-1. *J. Bone Miner. Res.* **19**, 841-852.

Badde, A. and Schulte, D. (2008). A role for receptor protein tyrosine phosphatase lambda in midbrain development. *J. Neurosci.* **28**, 6152-6164.

Badde, A., Bumsted-O'Brien, K. M. and Schulte, D. (2005). Chick receptor protein tyrosine phosphatase lambda/psi (cRPTPlambda/cRPTPpsi) is dynamically expressed at the midbrain-hindbrain boundary and in the embryonic neural retina. *Gene Expr. Patterns* **5**, 786-791.

Baik, J. H., Picetti, R., Saiardi, A., Thiriet, G., Dierich, A., Depaulis, A., Le Meur, M. and Borrelli, E. (1995). Parkinsonian-like locomotor impairment in mice lacking dopamine D2 receptors. *Nature* **377**, 424-428.

Bauer, M., Szulc, J., Meyer, M., Jensen, C. H., Terki, T. A., Meixner, A., Kinkl, N., Gasser, T., Aebischer, P. and Ueffing, M. (2008). Delta-like 1 participates in the specification of ventral midbrain progenitor derived dopaminergic neurons. *J. Neurochem.* **104**, 1101-1115.

Castillo, S. O., Baffi, J. S., Palkovits, M., Goldstein, D. S., Kopin, I. J., Witta, J., Magnuson, M. A. and Nikodem, V. M. (1998). Dopamine biosynthesis is selectively abolished in substantia nigra/ventral tegmental area but not in hypothalamic neurons in mice with targeted disruption of the Nurr1 gene. *Mol. Cell. Neurosci.* **11**, 36-46.

Castro, D. S., Hermanson, E., Joseph, B., Wallen, A., Aarnisalo, P., Heller, A. and Perlmann, T. (2001). Induction of cell cycle arrest and morphological differentiation by Nurr1 and retinoids in dopamine MN9D cells. *J. Biol. Chem.* **276**, 43277-43284.

Chen, W. L., Lin, J. W., Huang, H. J., Wang, S. M., Su, M. T., Lee-Chen, G. J., Chen, C. M. and Hsieh-Li, H. M. (2008). SCA8 mRNA expression suggests an antisense regulation of KLHL1 and correlates to SCA8 pathology. *Brain Res.* **1233**, 176-184.

Christophersen, N. S., Grønborg, M., Petersen, T. N., Fjord-Larsen, L., Jørgensen, J. R., Juliusson, B., Blom, N., Rosenblad, C. and Brundin, P. (2007). Midbrain expression of Delta-like 1 homologue is regulated by GDNF and is associated with dopaminergic differentiation. *Exp. Neurol.* **204**, 791-801.

Colebrooke, R. E., Humby, T., Lynch, P. J., McGowan, D. P., Xia, J. and Emson, P. C. (2006). Age-related decline in striatal dopamine content and motor performance occurs in the absence of nigral cell loss in a genetic mouse model of Parkinson's disease. *Eur. J. Neurosci.* **24**, 2622-2630.

Enomoto, H., Furuichi, T., Zanma, A., Yamana, K., Yoshida, C., Sumitani, S., Yamamoto, H., Enomoto-Iwamoto, M., Iwamoto, M. and Komori, T. (2004). Runx2 deficiency in chondrocytes causes adipogenic changes *in vitro*. *J. Cell Sci.* **117**, 417-425.

Giros, B., Jaber, M., Jones, S. R., Wightman, R. M. and Caron, M. G. (1996). Hyperlocomotion and indifference to cocaine and amphetamine in mice lacking the dopamine transporter. *Nature* **379**, 606-612.

Hansen, L. H., Madsen, B., Teisner, B., Nielsen, J. H. and Billestrup, N. (1998). Characterization of the inhibitory effect of growth hormone on primary preadipocyte differentiation. *Mol. Endocrinol.* **12**, 1140-1149.

He, Y., Zu, T., Benzow, K. A., Orr, H. T., Clark, H. B. and Koob, M. D. (2006). Targeted deletion of a single Sca8 ataxia locus allele in mice causes abnormal gait, progressive loss of motor coordination, and Purkinje cell dendritic deficits. *J. Neurosci.* **26**, 9975-9982.

Hurd, Y. L., Pristupa, Z. B., Herman, M. M., Niznik, H. B. and Kleinman, J. E. (1994). The dopamine transporter and dopamine D2 receptor messenger RNAs are differentially expressed in limbic- and motor-related subpopulations of human mesencephalic neurons. *Neuroscience* **63**, 357-362.

Izumi, Y., Maruyama, H., Oda, M., Morino, H., Okada, T., Ito, H., Sasaki, I., Tanaka, H., Komure, O., Udaka, F. et al. (2003). SCA8 repeat expansion: large CTA/CTG repeat alleles are more common in ataxic patients, including those with SCA6. *Am. J. Hum. Genet.* **72**, 704-709.

Jacobs, F. M. J., Smits, S. M., Hornman, K. J., Burbach, J. P. and Smidt, M. P. (2006). Strategies to unravel molecular codes essential for the development of meso-diencephalic dopaminergic neurons. *J. Physiol.* **575**, 397-402.

Jacobs, F. M. J., Smits, S. M., Noorlander, C. W., von Oerthel, L., van der Linden, A. J. A., Burbach, J. P. H. and Smidt, M. P. (2007). Retinoic acid counteracts developmental defects in the substantia nigra caused by *Pitx3*-deficiency. *Development* **134**, 2673-2684.

Jacobs, F. M. J., van Erp, S., van der Linden, A. J. A., von Oerthel, L., Burbach, J. P. H. and Smidt, M. P. (2009). Pitx3 potentiates Nurr1 in dopamine neuron terminal differentiation through release of SMRT-mediated repression. *Development* **136**, 531-540.

Jain, S., Golden, J. P., Wozniak, D., Pehek, E., Johnson, E. M., Jr, and Milbrandt, J. (2006). RET is dispensable for maintenance of midbrain dopaminergic neurons in adult mice. *J. Neurosci.* **26**, 11230-11238.
Jensen, C. H., Meyer, M., Schroder, H. D., Kliem, A., Zimmer, J. and Teisner, B. (2001). Neurons in the monoaminergic nuclei of the rat and human central nervous system express FA1/dlk. *NeuroReport* **12**, 3959-3963.
Kawano, H., Ohyama, K., Kawamura, K. and Nagatsu, I. (1995). Migration of dopaminergic neurons in the embryonic mesencephalon of mice. *Brain Res. Dev. Brain Res.* **86**, 101-113.
Kramer, E. R., Aron, L., Ramakers, G. M., Seitz, S., Zhuang, X., Beyer, K., Smidt, M. P. and Klein, R. (2007). Absence of Ret signaling in mice causes progressive and late degeneration of the nigrostriatal system. *PLoS Biol.* **5**, e39.
Law, S. W., Conneely, O. M., DeMayo, F. J. and O'Malley, B. W. (1992). Identification of a new brain-specific transcription factor, NURR1. *Mol. Endocrinol*. **6**, 2129-2135.
Li, L., Su, Y., Zhao, C., Zhao, H., Liu, G., Wang, J. and Xu, Q. (2006). The role of Ret receptor tyrosine kinase in dopaminergic neuron development. *Neuroscience* **142**, 391-400.
Megason, S. G. and McMahon, A. P. (2002). A mitogen gradient of dorsal midline Wnts organizes growth in the CNS. *Development* **129**, 2087-2098.
Moon, Y. S., Smas, C. M., Lee, K., Villena, J. A., Kim, K. H., Yun, E. J. and Sul, H. S. (2002). Mice lacking paternally expressed Pref-1/Dlk1 display growth retardation and accelerated adiposity. *Mol. Cell. Biol.* **22**, 5585-5592.
Mooslehner, K. A., Chan, P. M., Xu, W., Liu, L., Smadja, C., Humby, T., Allen, N. D., Wilkinson, L. S. and Emson, P. C. (2001). Mice with very low expression of the vesicular monoamine transporter 2 gene survive into adulthood: potential mouse model for parkinsonism. *Mol. Cell. Biol.* **21**, 5321-5331.
Nemes, J. P., Benzow, K. A., Moseley, M. L., Ranum, L. P. and Koob, M. D. (2000). The SCA8 transcript is an antisense RNA to a brain-specific transcript encoding a novel actin-binding protein (KLHL1). *Hum. Mol. Genet.* **9**, 1543-1551.
Paul, S. and Lombroso, P. J. (2003). Receptor and nonreceptor protein tyrosine phosphatases in the nervous system. *Cell. Mol. Life Sci.* **60**, 2465-2482.
Roepman, P., Wessels, L. F. A., Kettelarij, N., Kemmeren, P., Miles, A. J., Lijnzaad, P., Tilanus, M. G. J., Koole, R., Hordijk, G., Van der Vliet, P. C. et al. (2005). An expression profile for diagnosis of lymph node metastases from primary head and neck quamous cell carcinomas. *Nat. Genet.* **37**, 182-186.
Saucedo-Cardenas, O., Quintana-Hau, J. D., Le, W. D., Smidt, M. P., Cox, J. J., De Mayo, F., Burbach, J. P. H. and Conneely, O. M. (1998). Nurr1 is essential for the induction of the dopaminergic phenotype and the survival of ventral mesencephalic late dopaminergic precursor neurons. *Proc. Natl. Acad. Sci. USA* **95**, 4013-4018.
Seng, S., Avraham, H. K., Jiang, S., Venkatesh, S. and Avraham, S. (2006). KLHL1/MRP2 mediates neurite outgrowth in a glycogen synthase kinase 3beta-dependent manner. *Mol. Cell. Biol.* **26**, 8371-8384.
Shults, C. W., Hashimoto, R., Brady, R. M. and Gage, F. H. (1990). Dopaminergic cells align along radial glia in the developing mesencephalon of the rat. *Neuroscience* **38**, 427-436.
Simon, H. H., Bhatt, L., Gherbassi, D., Sgadó, P. and Alberí, L. (2003). Midbrain dopaminergic neurons: determination of their developmental fate by transcription factors. *Ann. New York Acad. Sci.* **991**, 36-47.
Smas, C. M., Chen, L., Zhao, L., Latasa, M. J. and Sul, H. S. (1999). Transcriptional repression of pref-1 by glucocorticoids promotes 3T3-L1 adipocyte differentiation. *J. Biol. Chem*. **274**, 12632-12641.
Smidt, M. P., Asbreuk, C. H., Cox, J. J., Chen, H., Johnson, R. L. and Burbach, J. P. (2000). A second independent pathway for development of mesencephalic dopaminergic neurons requires Lmx1b. *Nat. Neurosci.* **3**, 337-341.
Smidt, M. P., Smits, S. M., Bouwmeester, H., Hamers, F. P. T., van der Linden, A. J. A., Hellemons, A. J. C. G. M., Graw, J. and Burbach, J. P. H. (2004). Early developmental failure of substantia nigra dopamine neurons in mice lacking the homeodomain gene Pitx3. *Development* **131**, 1145-1155.
Smits, S. M., Ponnio, T., Conneely, O. M., Burbach, J. P. and Smidt, M. P. (2003). Involvement of Nurr1 in specifying the neurotransmitter identity of ventral midbrain dopaminergic neurons. *Eur. J. Neurosci.* **18**, 1731-1738.
Stepanek, L., Stoker, A. W., Stoeckli, E. and Bixby, J. L. (2005). Receptor tyrosine phosphatases guide vertebrate motor axons during development. *J. Neurosci.* **25**, 3813-3823.
Stoker, A. and Dutta, R. (1998). Protein tyrosine phosphatases and neural development. *BioEssays* **20**, 463-472.
Tornqvist, N., Hermanson, E., Perlmann, T. and Stromberg, I. (2002). Generation of tyrosine hydroxylase-immunoreactive neurons in ventral mesencephalic tissue of *Nurr1*$^{-/-}$ mice. *Brain Res. Dev. Brain Res.* **133**, 37-47.
Wallen, A., Zetterstrom, R. H., Solomin, L., Arvidsson, M., Olson, L. and Perlmann, T. (1999). Fate of mesencephalic *AHD2*-expressing dopamine progenitor cells in NURR1 mutant mice. *Exp. Cell Res.* **253**, 737-746.
Witta, J., Baffi, J. S., Palkovits, M., Mezey, E., Castillo, S. O. and Nikodem, V. M. (2000). Nigrostriatal innervation is preserved in *Nurr1*-null mice, although dopaminergic neuron precursors are arrested from terminal differentiation. *Brain Res. Mol. Brain Res.* **84**, 67-78.
Worth, P. F., Houlden, H., Giunti, P., Davis, M. B. and Wood, N. W. (2000). Large, expanded repeats in SCA8 are not confined to patients with cerebellar ataxia. *Nat. Genet.* **24**, 214-215.
Wu, H., Kerr, M. K., Cui, X. and Churchill, G. A. (2002). MAANOVA: a software package for the analysis of spotted cDNA microarray experiments. The analysis of gene expression data: methods and software, http://research.jax.org/faculty/churchill.
Wu, Y. R., Lin, H. Y., Chen, C. M., Gwinn-Hardy, K., Ro, L. S., Wang, Y. C., Li, S. H., Hwang, J. C., Fang, K., Hsieh-Li, H. M. et al. (2004). Genetic testing in spinocerebellar ataxia in Taiwan: expansions of trinucleotide repeats in SCA8 and SCA17 are associated with typical Parkinson's disease. *Clin. Genet.* **65**, 209-214.
Yan, H. X., He, Y. Q., Dong, H., Zhang, P., Zeng, J. Z., Cao, H. F., Wu, M. C. and Wang, H. Y. (2002). Physical and functional interaction between receptor-like protein tyrosine phosphatase PCP-2 and beta-catenin. *Biochemistry* **41**, 15854-15860.
Yan, H. X., Yang, W., Zhang, R., Chen, L., Tang, L., Zhai, B., Liu, S. Q., Cao, H. F., Man, X. B., Wu, H. P. et al. (2006). Protein-tyrosine phosphatase PCP-2 inhibits beta-catenin signaling and increases E-cadherin-dependent cell adhesion. *J. Biol. Chem.* **281**, 15423-15433.
Zetterström, R. H., Williams, R., Perlmann, T. and Olson, L. (1996). Cellular expression of the immediate early transcription factors Nurr1 and NGFI-B suggests a gene regulatory role in several brain regions including the nigrostriatal dopamine system. *Brain Res. Mol. Brain Res.* **41**, 111-120.
Zetterström, R. H., Solomin, L., Jansson, L., Hoffer, B. J., Olson, L. and Perlmann, T. (1997). Dopamine neuron agenesis in *Nurr1*-deficient mice. *Science* **276**, 248-250.
Zhou, Q. Y. and Palmiter, R. D. (1995). Dopamine-deficient mice are severely hypoactive, adipsic, and aphagic. *Cell* **83**, 1197-1209.